Hindawi
Complexity
Volume 2020, Article ID 1094386, 10 pages
https://doi.org/10.1155/2020/1094386

Research Article

First-Order and High-Order Repetitive Control for Single-Phase Grid-Connected Inverter

Cheng Guo,[1] **Linzhen Zhong**,[2] **Jun Zhao**,[2] **Guanbin Gao**,[2] **and Yingbo Huang**[2]

[1]*Yunnan Electrical Power Experiment Institute, Co., Kunming, Yunnan 650217, China*
[2]*Faculty of Mechanical and Electrical Engineering, Kunming University of Science and Technology, Kunming 650500, China*

Correspondence should be addressed to Jun Zhao; junzhao1993@163.com

Received 19 June 2020; Revised 11 July 2020; Accepted 16 July 2020; Published 12 August 2020

Guest Editor: Shubo Wang

With the increasing demand of users for power sources and quality, how to provide high-quality renewable clean energy has become a key issue of power electronics. The main idea of this paper is to develop a composite control including a PI control and repetitive control for a single-phase grid-connected inverter to eliminate the effects of harmonics, which can obtain better steady-state and dynamic responses of the single-phase inverter system and reduce the net current harmonics. The modelling of a single-phase inverter is first introduced; then a first-order repetitive control is developed for the proposed grid-connected inverter. Moreover, a high-order repetitive controller is adopted to further improve the robustness against the uncertainties in the period of signals. The stability and performance analysis are given for the first-order repetitive control and high-order repetitive control. Finally, comparative simulations are conducted in a circuit-level inverter model, which show the effectiveness of the proposed method.

1. Introduction

The development of traditional fuel-based energy is becoming stringent due to its serious pollution problem and other shortcomings, while with the rapid development of human economy and society, the investigation of clean and high-efficiency energy has been gradually expanded [1, 2]. In fact, the exploration of renewable energy and alternative energy has been gradually becoming a key research area in various countries and industries. In the fields of power generation, thermal power is now being gradually replaced by renewable energy such as hydropower, photovoltaic and wind power, nuclear energy, and solar energy [3, 4].

However, there are some critical issues to be addressed in the renewable energy powered grid-connected systems. For instance, photovoltaic power generation is greatly affected by many factors such as weather and region, and thus the power supply is not stable [3, 5]. In addition, due to the characteristics of large investment and wide land occupation, the centralized photovoltaic grid-connected system has limited application, though the distributed photovoltaic grid-connected system has more potential applications, that is, small-scale photovoltaic grid-connected system. However, it remains as an open problem to ensure that a large number of distributed systems can be successfully connected to the grid through power electronic methods, that is, grid-connected inverter [6–9], which can retain the stability of public grid while ensuring the efficiency of the grid connection and avoiding the interference of large-scale grid connection to public grid. This is of great significance and necessity not only for the photovoltaic power generation system but also for other renewable energy powered systems [5]. Among these grid-connected systems, the grid-connected inverter is the core part [10–12]. As an interface device, the grid-connected inverter used to transform the unstable DC power received by photovoltaic cells into a more stable AC power supply and feed it into the public grid plays an important role, which has also attracted significant attentions in the power electronics industry [13–15].

The grid-connected inverter is to convert the DC power output extracted from the photovoltaic array into the AC power with the same frequency and phase as the grid voltage,

while the output current harmonic should be small and the sinusoidal AC is incorporated into the grid. Hence, proper control strategies are essential for this purpose. There are two basic control strategies of the grid-connected current, that is, indirect current control and direct current control [16–19]. Indirect current control uses the vector relationship of the output voltage, so that the grid-connected current can achieve the expected amplitude and phase, without the introduction of AC current feedback. Direct current control applies the AC input current command and AC current feedback, so as to make the input current tracking command change through the regulator's tracking control; it has good dynamic performance. In this line, there are many control methods developed for grid-connected inverter, such as PI control, hysteresis control, deadbeat control, robust control, repetitive control, and adaptive control [20–26]. PI control is one of the commonly used control methods since this algorithm is simple and reliable, but it cannot realize the current adjustment without static difference. It may contain oscillations, so that the current quality of the network side is limited. Hysteresis control is designed to control the error of the inverter output current to track a sinusoidal reference current within the hysteresis width, which has the advantages of real-time control and fast response. However, this method suffers the problems of switching loss and tracking accuracy. Deadbeat control is a method based on the precise mathematical model of the controlled plant. The basic principle is to calculate the duty cycle of the next switching cycle of the inverter power device according to the state equation and the output feedback signal and the required reference signal at the next time. Deadbeat control has the advantages of fast response and low harmonic content. However, it has specific requirements for the calculation accuracy and speed of the controller.

Based on the above discussions, we will develop a repetitive control for a grid-connected inverter. Repetitive control is a control method developed based on the internal model principle, where the basic principle is that the harmonic distortion of the previous cycle will be eliminated in the next cycle. The controller is used to add control signals in the next cycle for correction and compensation, so as to eliminate the periodic interference. To this end, we first introduce the modelling of a single-phase inverter. Then, a first-order repetitive control is developed for the proposed grid-connected inverter. Moreover, a high-order repetitive controller is also adopted to further improve the robustness against the uncertainties in the period of signals. The stability and performance analysis are all given for the proposed two control strategies. Finally, comparative simulations are conducted in a circuit-level inverter model to show that the high-order repetitive control can obtain better steady-state and dynamic features of the single-phase inverter system and reduce the net current harmonics.

The major contributions of this paper include the following:

(1) The repetitive control is used to eliminate the total harmonics in the current of the grid-connected inverter

(2) A high-order repetitive control is proposed to address the variation in the period of grid, which can guarantee the control system robustness of the grid-connected inverter

(3) The stability and performance analysis for the proposed first-order repetitive control and high-order repetitive control are all given

This paper is organized as follows: In Section 2, we introduce the single-phase inverter type and modelling. In Section 3, a first-order repetitive control and high-order repetitive control are introduced based on the proposed grid-connected inverter to suppress the total harmonics in the current. The stability and performance analysis are also given. Comparative simulations are conducted in Section 4, and some conclusions are stated in Section 5.

2. Preliminaries and Problem Formulation

2.1. Single-Phase Inverter Type. Grid-connected inverter is the poststage structure of photovoltaic grid, which is a device to convert DC into AC. Inverters are widely used in the electric, traffic, military, and other fields. There are three main topologies of single-phase inverter: push-pull inverter, half-bridge inverter, and full-bridge inverter [27–31].

2.1.1. Push-Pull Inverter. The push-pull inverter has a simple structure, which consists of two common negative power switches and a step-up transformer with a central tap on its original side. The main disadvantage is that the output transformer is easy to saturate. The utilization ratio of transformer is relatively low, and it is difficult to drive the inductive load, which is suitable for the occasion of low DC bus voltage. The topology of push-pull inverter is given in Figure 1.

2.1.2. Half-Bridge Inverter. The half-bridge inverter circuit is composed of two capacitors in series, a pair of controllable devices, and a bridge arm for antiparallel diodes. When the capacity of the two voltage dividing capacitors is large enough, the capacitor voltage of the power switch device keeps $U_d/2$ when being in switching on and off state, which has a strong ability to resist voltage output imbalance. However, its disadvantage is that the AC output voltage amplitude of the main circuit is half of the input voltage, and the DC side still needs the voltage balance of two capacitors, the DC side voltage utilization is low, and the harmonic of the grid current is large. Half-bridge inverter has been widely used in the low power level inverter. The topology of half-bridge inverter is shown in Figure 2.

2.1.3. Full-Bridge Inverter. The full-bridge inverter circuit has two bridge arms, which can be composed of two half-bridge circuits. The topology is given in Figure 3. One pair of full-control devices is V_1 and V_4, and the other pair is V_2 and V_3. The same pair of full-control devices is on at the same time, and the two pairs of devices are complementary.

Under the same DC input voltage, the maximum output voltage of the full-bridge inverter is twice of that of the half-bridge inverter. When the power is the same, the output

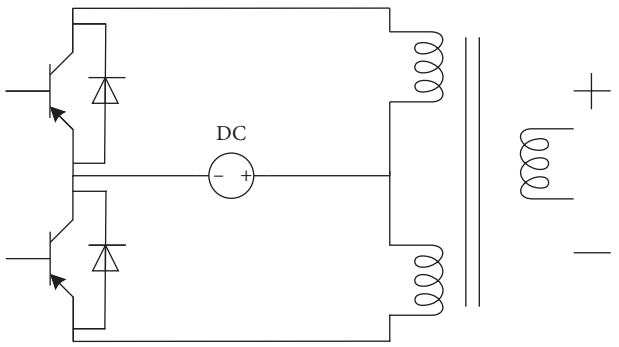

Figure 1: Push-pull inverter circuit.

current and the current through the switch element are half of the half-bridge inverter circuit. Full-bridge inverter circuit is simple in terms of structure and easy to control; therefore, it has been widely used in the high-power occasions.

At the same time, the inverter is divided into the active inverter and passive inverter according to whether there is a power supply or not. Active and passive refer to whether the inverter is connected to the power supply. In this project, the photovoltaic grid-connected inverter needs to be connected to the grid, which belongs to the grid-connected inverter, so that the active inverter circuit is selected.

From Figure 3, for the inverter with load, its filter circuit is usually composed of an LC filter circuit with inductance and capacitance. For the grid-connected inverter, the output terminal needs to be connected to the grid. The filter capacitor C will be clamped by the power grid and cannot play the role of filtering, and the parallel capacitor can be removed equivalently, which can be seen in Figure 4.

This paper mainly focusses on the later stage of the grid-connected inverter system, which consists of a DC power supply provided by the former DC-DC part, four power switch devices (IGBT) inverter bridge, and filter inductor. The inverter outputs sinusoidal current with the same frequency and phase the same as the grid voltage and enters the grid.

2.2. Modelling of Single-Phase Inverter. The main circuit of the single-phase grid-connected inverter is shown in Figure 5, which is a voltage type full-bridge circuit composed of four IGBTs and continuous current diodes in reverse parallel. $T_1 - T_4$ is the IGBT, $\mathrm{VD}_1 - \mathrm{VD}_4$ is the continuous current diode, L_s is the filter inductance on one side of the power grid, and R_s is the parasitic resistance of the filter inductance. U_s and U_{dc} are the corresponding AC power supply and DC power supply, respectively.

According to Figure 5, we can obtain the flowing equation:

$$L_s \frac{\mathrm{d}i_s}{d_t} = U_{AB} - U_s - R_s i_s. \tag{1}$$

Then, we have

$$\frac{I_s(s)}{U_{\mathrm{AB}}(s) - U_s(s)} = \frac{1}{R_s + L_s s}. \tag{2}$$

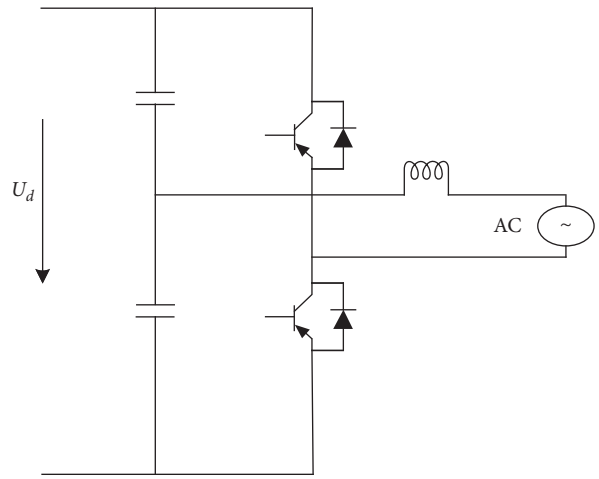

Figure 2: Half-bridge inverter circuit.

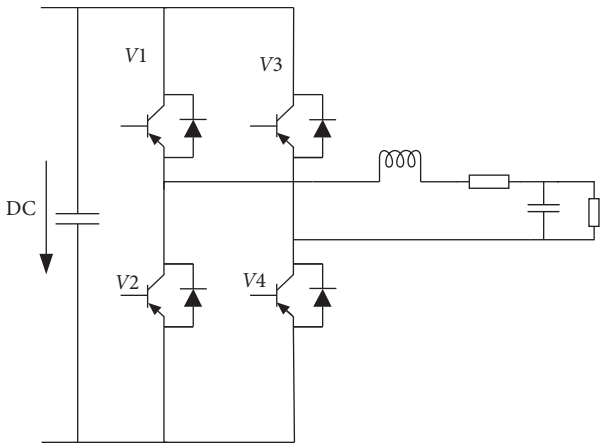

Figure 3: Full-bridge inverter circuit without AC.

For the DC side, we get

$$\frac{U_{\mathrm{dc}}(s)}{I_{\mathrm{dc}}(s) - I_L(s)} = \frac{1}{sC_{\mathrm{dc}}}. \tag{3}$$

Then, we know that the single-phase grid-connected inverter adopts the double loop control strategy of voltage and current loop, and the outer loop is the DC side voltage loop, whose function is to keep the DC side voltage stable. The inner loop is a current loop, the output current of the inverter is in the same phase as the grid voltage, and the current amplitude is determined by the output of the voltage loop regulator. This paper only studies the inverter function of the later stage of the grid-connected system; therefore, the front end of the inverter bridge can be regarded as a constant voltage DC power supply, while the voltage loop is not considered.

3. Repetitive Control Design of Single-Phase Grid-Connected Inverter

Repetitive control [32] is derived from the internal model principle (IMP). The merit of IMP is that, in a stable closed-loop control system, the internal control includes the

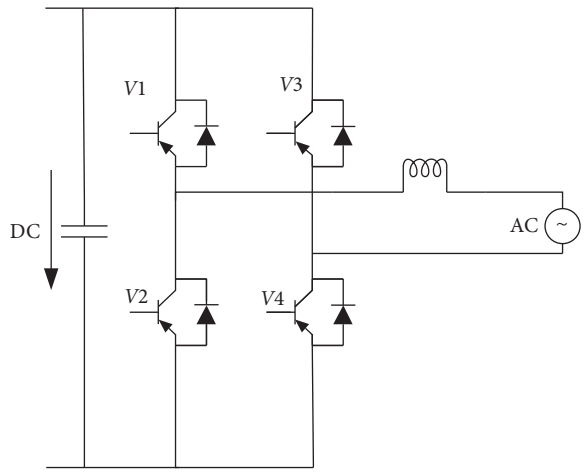

Figure 4: Full-bridge inverter circuit with AC.

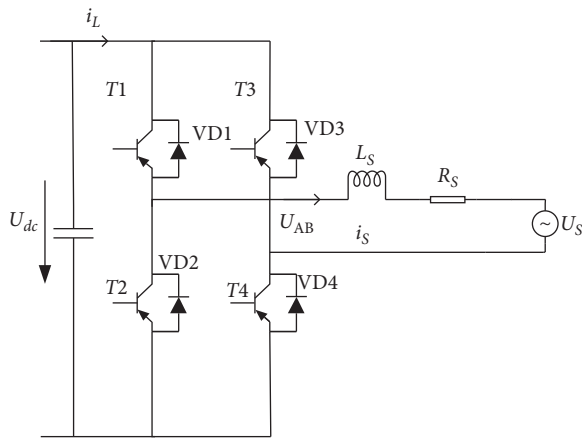

Figure 5: The main circuit of single phase.

generator of external controlled signals, so as to realize the adjustment without steady-state error and suppress the periodic interference. When the steady-state error of a system is zero, thus the input of the controller is zero. At this time, the reference signal and the feedback signal still exist, the periodic disturbance still changes according to the original dynamic characteristics, and the controller still outputs the corresponding control signal to keep the system adjusted without static error. Therefore, the essence of realizing no steady-state error is that the controller is a structural model, which can reflect and process external signals.

The proposed controller should be designed to suppress the current harmonics to reduce the distortion of sine wave of current feed into the network. However, the jamming signal in the power electronic system is periodic; then a particular control structure shown in Figure 6 will be used.

Remark 1. This control system in Figure 6 consists of an RC controller and PI controller. The PI controller is designed to stabilize the closed-loop system, whose parameters can be tuned as [33]. This paper will focus on the design of

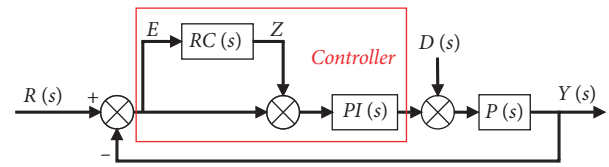

Figure 6: Schematic of the proposed control.

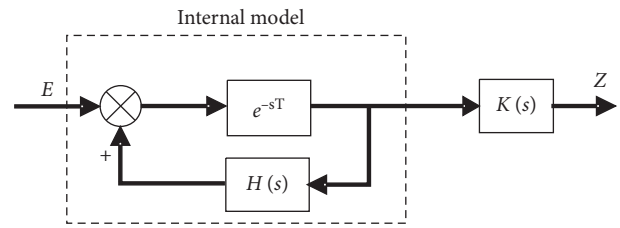

Figure 7: Block diagram of FORC.

repetitive control (e.g., FORC and HORC) and their comparisons.

3.1. First-Order Repetitive Control (FORC)

3.1.1. First-Order Repetitive Control Structure. As shown in Figure 7, repetitive control can be designed based on an internal model, which can learn a signal of the period T and duplicate it, even if the input of this model is set to zero. Consider the frequency-domain response; this internal model introduces infinite gains (without filter $H(s)$) at the specific frequencies $\omega = 2n\pi/T$ rad/s $\forall n \in N^+$. Then, according to the well-known IMP, zero-error tracking or rejection of period signals at these frequencies can be guaranteed if the closed-loop system is stable.

A low-pass filter $H(s)$ is usually used to improve the robustness of controlled systems, although it may reduce the gains in these specific frequencies. $H(s)$ is set as a second-order Butterworth filter in this paper by designing its cut-off frequency. The compensator $K(s)$ is utilized to retain the system stability when the internal model is added to the closed-loop system. Thus, the transfer function of RC is described by

$$\mathrm{RC}(s) = \frac{Z(s)}{E(s)} = \frac{e^{-\mathrm{sT}}}{1 - H(s)e^{-\mathrm{sT}}} \cdot K(s). \tag{4}$$

It is found that the use of low-pass filter $H(s)$ will lead to an unavoidable phase lag, which will shift the frequencies at which the maximum gains are obtained. Specifically, the frequency shift is mainly related to its phase. However, a proper compensation can be further incorporated to address this issue as [34].

3.1.2. Stability and Performance Analysis. In this part, we will give a proposition regarding the system stability. The following conditions should be fulfilled to guarantee the stability of the closed-loop system.

Proposition 1. *The closed-loop system in Figure 6 with FORC in Figure 7 is stable if the following conditions are fulfilled [35, 36]:*

(1) The closed-loop system without RC is stable; that is, $T_0(s) = PI(s)P(s)/(1 + PI(s)P(s))$ *is stable*

(2) $\|H(s)\|_\infty \le 1$*; that is, the filter should have a gain close to 1 within the suitable bandwidth*

(3) $\|(K(s)T_0(s) - H(s))e^{-sT}\|_\infty = \|K(s)T_0(s) - H(s)\|_\infty \le 1.$

Proof. The proof is similar to that given in [36] and thus is not presented here.

According to these three conditions, we have different design methods to satisfy the conditions. The PI control is designed to fulfill condition (1), a low-pass filter $H(s)$ is used to fulfill condition (2), and $K(s)$ can be designed to satisfy condition (3). For any minimum-phase plant $P(s)$, a constructive selection of $K(s)$ is given as

$$K(s) = k_r H(s)/T_0(s), \tag{5}$$

where k_r is a constant.

By substituting (5) into condition (3) of Proposition 1, we have the following. □

Corollary 1. *The closed-loop control system shown in Figure 6 with a stable minimum-phase* $P(s)$ *and compensator (5) is stable if the following conditions are fulfilled:*

(1) $H(s)$ *is a stable system,* $\|H(s)\|_\infty < 1$*(2)* k_r *is a constant fulfilling,* $|k_r - 1| < 1/\|H(s)\|_\infty$

Remark 1. The compensator $K(s)$ of (5) is valid for stable minimum-phase plants, because there are no zero-pole cancellations in the right-half plane in this case. For nonminimum-phase plants, an alternative approach is to cancel the minimum-phase zeroes and poles and to compensate for the phase of the nonminimum-phase ones as [37].

3.2. High-Order Repetitive Control (HORC)

3.2.1. High-Order Repetitive Control Structure. Although FORC in Figure 7 is easy to implement, its performance may degrade when the period T of the reference or disturbance has uncertainties; that is, it is sensitive to the variation in the period of signals. In order to tackle these disadvantages, high-order repetitive control (HORC) was proposed in [38–40] because of its strong robustness, which is given in Figure 8.

In Figure 8, $W(s)$ is a weighted sum function of repetitive loops. Thus, the transfer function of HORC can be written as

$$\mathrm{HORC}(s) = \frac{W(s)K(s)}{1 - W(s)H(s)}. \tag{6}$$

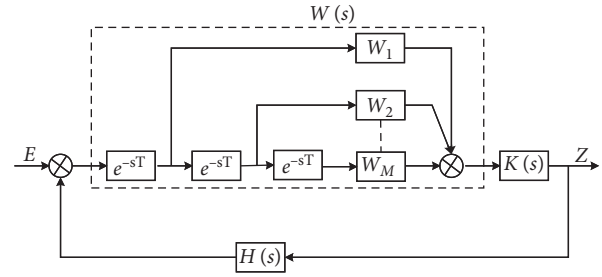

Figure 8: Block diagram of HORC.

It is shown that HORC uses a multiple loop internal model, which replaces the delay $e^{-\mathrm{sT}}$ by a weighted sum function of several delays given as follows:

$$W(s) = \sum_{m=1}^{M} W_m e^{-\mathrm{msT}}, \tag{7}$$

where M is the number of delays, that is, the order of RC loop.

Similar to FORC, the gains of HORC are infinite at the multiples of the input signal frequency. In particular, the gain of (6) will tend to infinity if $W(s)H(s) = 1$. As shown in [38], we substitute $s = jk2\pi/T$ into (7) and have

$$W(jk2\pi/T) = \sum_{m=1}^{M} W_m e^{-jmk2\pi} = \sum_{m=1}^{M} W_m = 1. \tag{8}$$

It is noted that, for $M = 1$ and $W_1 = 1$, (8) is reduced to FORC. For the case $M > 1$, we need to determine the weight parameters W_m. Inspired by the idea of [38], we can make the first-order derivative of $W(s)$ with respect to T zero at the specific frequency. This imposes the condition

$$\frac{\partial W(s = jk2\pi/T)}{\partial T} = \sum_{m=1}^{M} \frac{-W_m m jk2\pi}{T} = 0. \tag{9}$$

According to (9), the following equation is true:

$$\sum_{m=1}^{M} W_m m = 0. \tag{10}$$

As shown in [38], to further decrease the sensitivity for period-time variations by using the weight parameters of HORC, we can make $(M - 1)$-th derivatives equal zero, so that

$$\sum_{m=1}^{M} W_m m^{(M-1)} = 0. \tag{11}$$

The weight parameters can be calculated based on (7)–(11). For example, when $M = 2$ and 3, we can set $W_1 = 2$ and $W_2 = -1$; $W_1 = 3$, $W_2 = -3$, and $W_3 = 1$, respectively.

3.2.2. Stability and Performance Analysis. The stability analysis of HORC system is similar to that given in Proposition 1, and thus we have the following.

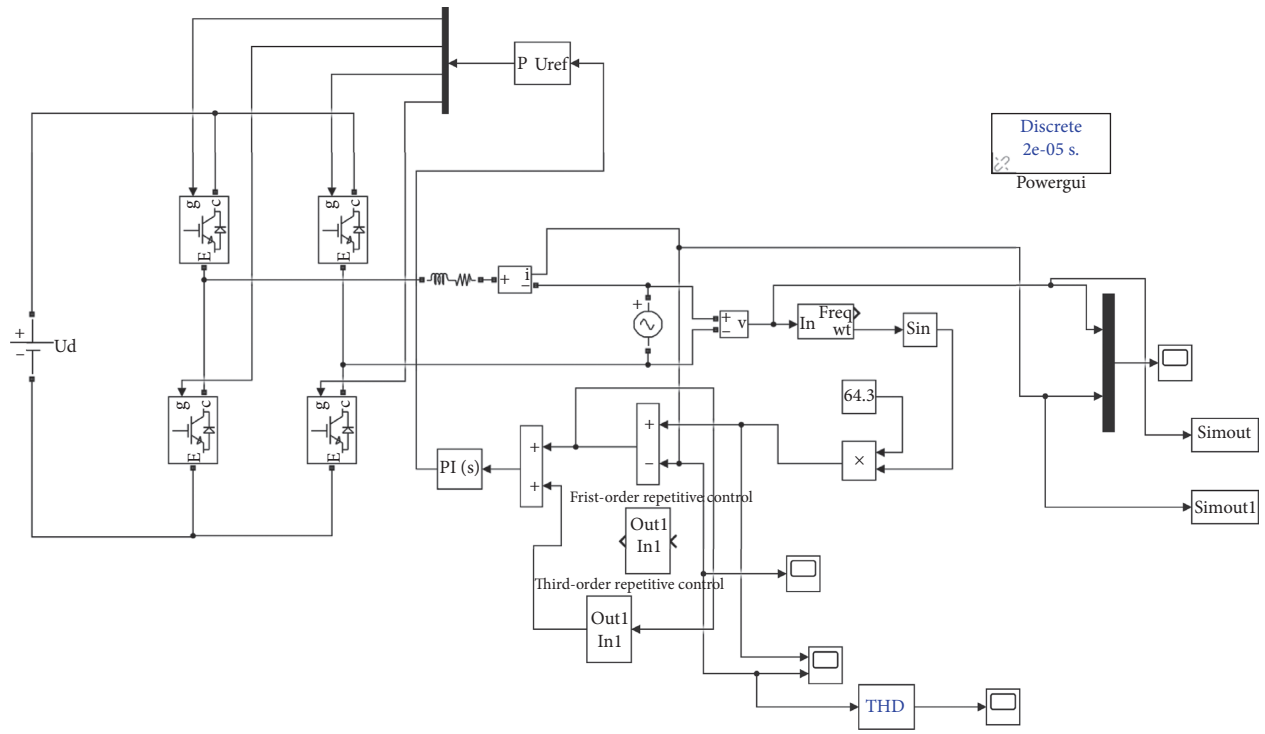

Figure 9: The simulation diagram of single-phase inverter.

Proposition 2. *The closed-loop system in Figure 6 with HORC in Figure 8 is stable if the following conditions hold:*

(1) The closed-loop system without the HORC is stable; that is, $T_0(s) = PI(s)P(s)/(1 + PI(s)P(s))$ *is stable*

(2) $\|H(s)\|_\infty \le 1$

(3) $\|(K(s)T_0(s) - H(s))W(s)\|_\infty \le 1$

Proof. The proof is similar to that of Proposition 1 by replacing e^{-sT} with $W(s)$.

For any minimum-phase $P(s)$, we design $K(s)$ as

$$K(s) = \frac{k_r H(s)}{T_0(s)}. \tag{12}$$

By substituting (12) into the third condition in Proposition 2, we can get. $\|(k_r H(s) - H(s))W(s)\|_\infty \le 1$. Furthermore, condition (2) in Corollary 2 can be derived as $|k_r - 1| < 1/\|H(s)W(s)\|_\infty$. Hence, we have the following. □

Corollary 2. *For stable, minimum-phase* $P(s)$*, the closed-loop control system shown in Figure 8 with HORC is stable if the following conditions are true:*

(1) $\|H(s)\|_\infty < 1$

(2) k_r *is a constant fulfilling* $|k_r - 1| < 1/\|H(s)W(s)\|_\infty$

4. Simulation Results and Analysis

In this section, we validate the effectiveness of the proposed control algorithms by using *Simpower systems Toolbox* in Matlab/Simulink. The simulation model of a single-phase grid-connected inverter is built to compare the current harmonic suppression of FORC and HORC. The FFT analysis tool in Simulink is used to get the total harmonic distortion (THD). Through the block diagram of current loop control system in Figure 6 and the topology structure in Figure 5 of the single-phase grid-connected inverter, the simulation diagram of the single-phase inverter can be obtained as Figure 9. In addition, the main circuit parameters are shown in Table 1.

The main circuit simulation module is composed of a DC power supply, an IGBT inverter bridge, a filter inductor, an AC source of public power grid, and an output current detection module. The control part consists of a control circuit, a PWM generator module, and a PLL module. The current loop is used in the control loop. The control module includes a PI control, a first-order repetitive control, or a high-order repetitive control, respectively. In this paper, PI control, PI + FORC, and PI + HORC are all simulated. In order to fully analyze the characteristics of these three control methods, the steady-state waveform, harmonic suppression, and dynamic tracking are all given.

4.1. The Steady-State Waveform. Figures 10–12 show the voltage and current of AC side when the PI control, PI + FORC, and PI + HORC reach the steady state, respectively. Figures 13–15 are the corresponding harmonic analysis results. It can be seen from Figures 10–12 that the three methods can achieve the same phase of voltage and current in the steady state. However, the current harmonic is relatively large and the THD reaches 2.10% in Figure 12. In Figure 11, the harmonics are correspondingly less and the THD is

Table 1: The simulation parameters.

Parameters	Values
Grid phase voltage U_s (V)	220
DC side voltage U_{DC} (V)	800
Switching frequency f_s (kHz)	10
Filter inductance L_s (mH)	30
Inductance equivalent resistance R_s (Ω)	0.1
Input voltage frequency f (Hz)	50

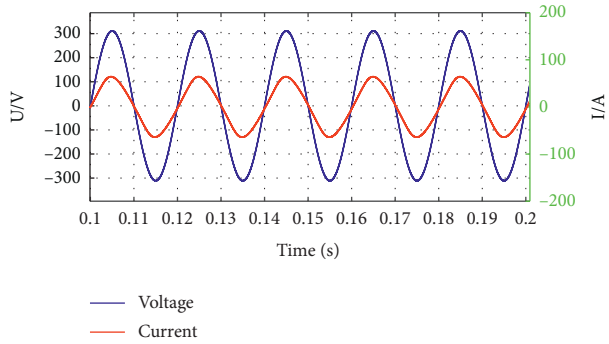

Figure 10: Simulation results of PI control.

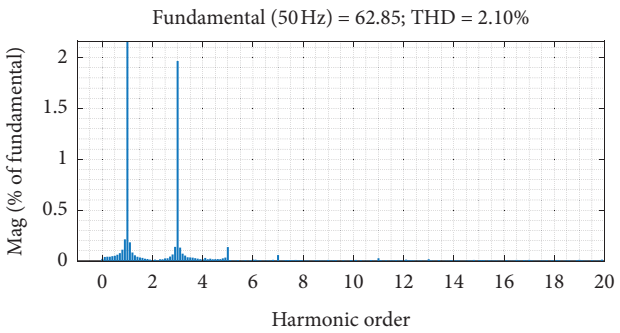

Figure 11: The THD of PI + FORC control.

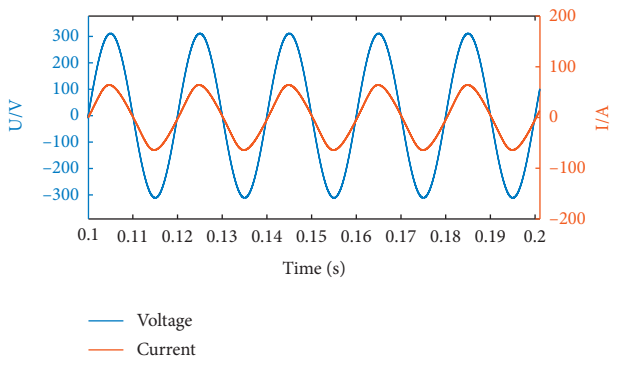

Figure 12: The THD of PI control.

reduced to 1.98% when PI + FORC is adopted. Finally, PI + HORC is used to suppress the current harmonics more restrictively, where the THD is reduced to 1.84% in Figure 15.

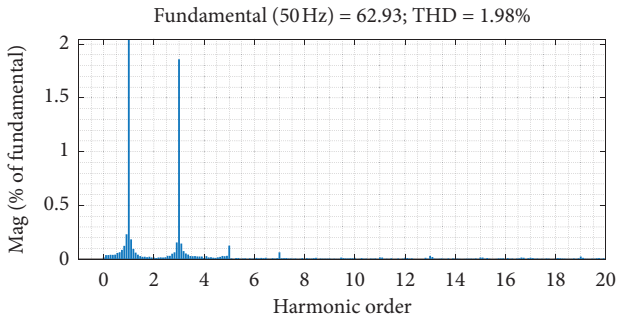

Figure 13: Simulation results of PI + HORC control.

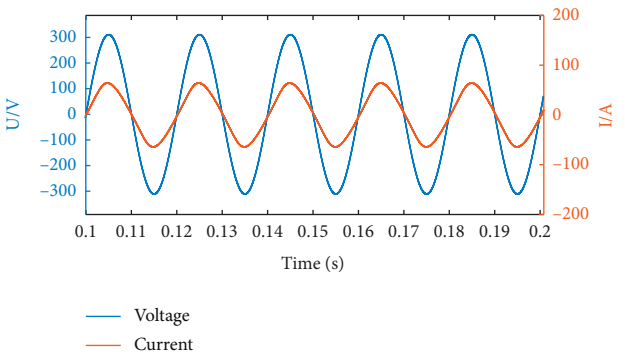

Figure 14: Simulation results of PI + FORC control.

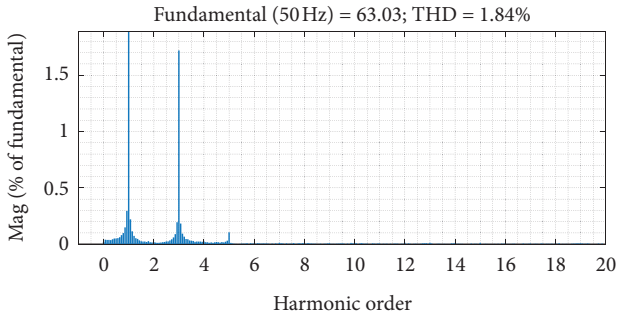

Figure 15: The THD of PI + HORC control.

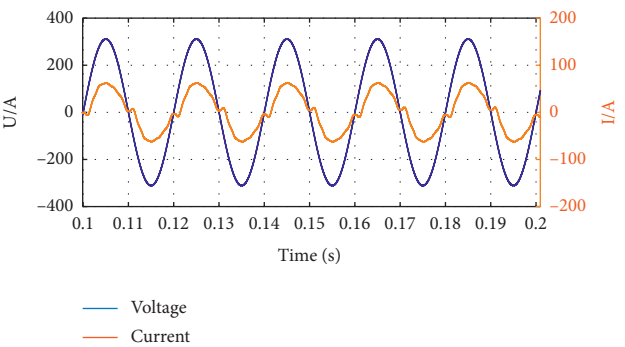

Figure 16: Simulation results of PI control with high-order harmonics.

4.2. Harmonic Suppression. In order to further verify the harmonic suppression of the three control methods, high-order harmonics are added to the system manually. The frequency of

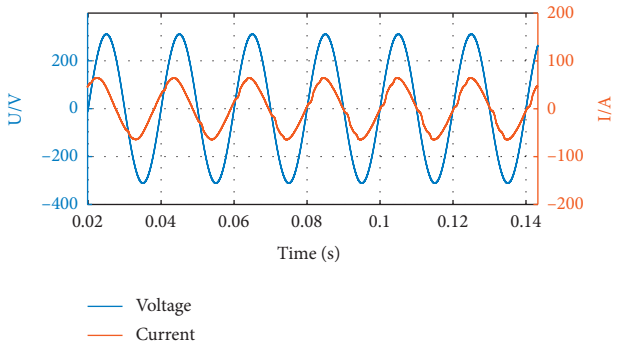

Figure 17: Simulation diagram of PI + FORC control with high-order harmonics.

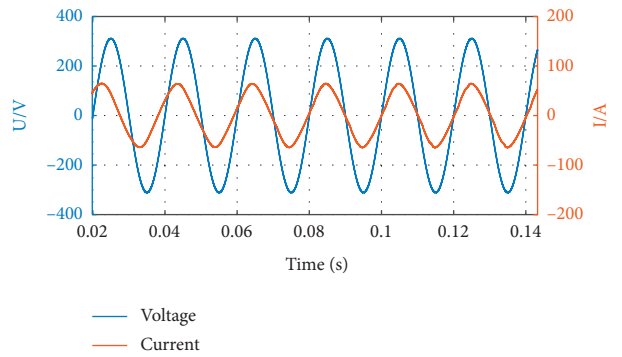

Figure 18: Simulation results of PI + HORC control with high-order harmonics.

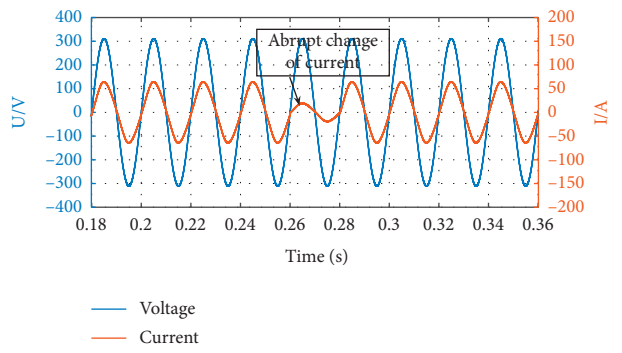

Figure 19: The simulation diagram when current breaks in PI + HORC control.

the grid is set as 50 Hz; then the 7th and 9th harmonics are injected. It is shown in Figure 16 that PI control has poor performance to suppress harmonics and it leads to great distortions in the current. It can be seen from Figure 17 that, after the introduction of FORC, the high-order harmonics are suppressed and the output current retains a better sinusoidal waveform. After using HORC, we can get a smoother sine curve, as shown in Figure 18.

4.3. Dynamic Tracking. Through the above analysis, we can find that the HORC has a better harmonic suppression performance. In order to further verify the tracking performance of HORC, the reference current is suddenly reduced by 30% in 0.26s to simulate the sudden drop of current. It is shown in Figure 19 that the current can be recovered in 0.28s. Therefore, when the reference current changes suddenly, the current can respond quickly, and the reference current can be tracked after a short transient; that is, the system has fast dynamic response.

5. Conclusion

In this paper, a novel control method combining PI control and repetitive control is proposed for a single-phase grid-connected inverter. After introducing the single-phase inverter type and modelling, a first-order repetitive control and a high-order repetitive control are developed for the grid-connected inverter, respectively. The stability and performance analysis are all given for the proposed two repetitive controls. Finally, comparative simulations are conducted based on the proposed single-phase grid-connected inverter to show that the high-order repetitive control can obtain better steady-state and dynamic features and reduce the net current harmonics. Future work will focus on the reactive power compensation control and its practical application.

Data Availability

The data used to support the findings of this study are available from the corresponding author upon request.

Conflicts of Interest

The authors declare that there are no conflicts of interest regarding the publication of this paper.

Acknowledgments

This work was supported by China Southern Power Grid Corporation (no. YNKJXM20180366) and the Scientific Research Fund of Yunnan Education Department under Grant 2020J0067.

References

[1] C. Zhang, Y. Ye, and H. Chen, "Photovoltaic grid connected inverter based on output current control," *Journal of Electrical Technology*, vol. 22, no. 8, pp. 41–45, 2007.

[2] F. Wang, S. Yu, and J. Su, "Research on solar photovoltaic grid connected power generation system," *Journal of Electrical Technology*, vol. 20, no. 5, pp. 72–74, 2005.

[3] Z. Yao, F. Yu, and Q. Zhao, "Simulation of large photovoltaic grid connected system based on modular multilevel converter," *Chinese Journal of Electrical Engineering*, vol. 33, no. 36, pp. 27–33, 2013.

[4] T. Cheng, M. Chen, Y. Wang et al., "Adaptive robust method for dynamic economic emission dispatch incorporating renewable energy and energy storage," *Complexity*, vol. 2018, Article ID 2517987, 13 pages, 2018.

[5] X. Guo, X. Zhang, Z. Lu, B. Wang, H. Qi, and X. Sun, "Power/current quality coordinated control strategy of photovoltaic grid connected inverter under unbalanced grid voltage,"

Chinese Journal of Electrical Engineering, vol. 34, no. 3, pp. 346–353, 2014.

[6] Z. Yao and L. Xiao, "Control of single-phase grid-connected inverters with nonlinear loads," *IEEE Transactions on Industrial Electronics*, vol. 60, no. 4, pp. 1384–1389, 2013.

[7] Q. Yan, X. Wu, X. Yuan, and Y. Geng, "An improved grid-voltage feedforward strategy for high-power three-phase grid-connected inverters based on the simplified repetitive predictor," *IEEE Transactions on Power Electronics*, vol. 31, no. 5, pp. 3880–3897, 2016.

[8] Y. He, H. S.-H. Chung, C.-T. Lai, X. Zhang, and W. Wu, "Active cancelation of equivalent grid impedance for improving stability and injected power quality of grid-connected inverter under variable grid condition," *IEEE Transactions on Power Electronics*, vol. 33, no. 11, pp. 9387–9398, 2018.

[9] C. Zhao, J. Liu, Z. Xie, and F. Zhou, "Coordinate control of power/current for grid-connected inverter based on PCI controller under unbalanced grid conditions," *Complexity*, vol. 2019, Article ID 5968984, 14 pages, 2019.

[10] Q. L. Zhao, X. Q. Guo, and W. Y. Wu, "Research on grid connected control technology of single-phase inverter," *Chinese Journal of Electrical Engineering*, vol. 27, no. 16, pp. 60–64, 2007.

[11] M. Dong and A. Luo, "Design and control method of inverter in photovoltaic grid connected power generation system," *Power System Automation*, vol. 30, no. 20, pp. 97–102, 2006.

[12] X. B. Ruan and Y. G. Yan, "Control strategy of four leg three-phase inverter," *Transactions of China Electrotechnical Society*, vol. 15, no. 1, pp. 61–64, 2000.

[13] B. Sahan, A. N. Vergara, N. Henze, A. Engler, and P. Zacharias, "A single-stage PV module integrated converter based on a low-power current-source inverter," *IEEE Transactions on Industrial Electronics*, vol. 55, no. 7, pp. 2602–2609, 2008.

[14] J. Selvaraj and N. A. Rahim, "Multilevel inverter for grid-connected PV system employing digital PI controller," *IEEE Transactions on Industrial Electronics*, vol. 56, no. 1, pp. 149–158, 2009.

[15] S. Wang, L. Tao, Q. Chen, J. Na, and X. Ren, "USDE-based sliding mode control for servo mechanisms with unknown system dynamics," *IEEE/ASME Transactions on Mechatronics*, vol. 25, no. 2, pp. 1056–1066, 2020.

[16] J. Fei, T. Li, F. Wang, and W. Juan, "A novel sliding mode control technique for indirect current controlled active power filter," *Mathematical Problems in Engineering*, vol. 2012, Article ID 549782, 18 pages, 2012.

[17] Y.-P. Liu, K.-Z. Liu, and X. Yang, "Nonlinear current control for reluctance actuator with hysteresis compensation," *Journal of Control Science and Engineering*, vol. 2014, Article ID 150345, 7 pages, 2014.

[18] G. Drexlin, V. Hannen, S. Mertens, and C. Weinheimer, "Current direct neutrino mass experiments," *Advances in High Energy Physics*, vol. 2013, Article ID 293986, 39 pages, 2013.

[19] M. Ruiz-Ruigomez, J. Badiola, S. M. Schmidt-Malan et al., "Direct electrical current reduces bacterial and yeast biofilm formation," *International Journal of Bacteriology*, vol. 2016, Article ID 9727810, 6 pages, 2016.

[20] R. Grino, R. Cardoner, R. Costa-Castello, and E. Fossas, "Digital repetitive control of a three-phase four-wire shunt active filter," *IEEE Transactions on Industrial Electronics*, vol. 54, no. 3, pp. 1495–1503, 2007.

[21] R. Costa-Castello, R. Grino, and E. Fossas, "Odd-harmonic digital repetitive control of a single-phase current active filter," *IEEE Transactions on Power Electronics*, vol. 19, no. 4, pp. 1060–1068, 2004.

[22] G. Weiss, Q.-C. Zhong, T. C. Green, and J. Liang, "Repetitive control of DC-AC converters in microgrids," *IEEE Transactions on Power Electronics*, vol. 19, no. 1, pp. 219–230, 2004.

[23] K. Zhou and D. Wang, "Digital repetitive learning controller for three-phase CVCF PWM inverter," *IEEE Transactions on Industrial Electronics*, vol. 48, pp. 820–830, 2001.

[24] S. Wang, J. Na, and Y. Xing, "Adaptive optimal parameter estimation and control of servo mechanisms: theory and experiments," *IEEE Transactions on Industrial Electronics*, vol. 99, p. 1, 2020.

[25] S. Wang and J. Na, "Parameter estimation and adaptive control for servo mechanisms with friction compensation," *IEEE Transactions on Industrial Informatics*, vol. 99, p. 1, 2020.

[26] J. Zhao, J. Na, and G. Gao, "Adaptive dynamic programming based robust control of nonlinear systems with unmatched uncertainties," *Neurocomputing*, vol. 395, pp. 56–65, 2020.

[27] P. Giri, A. Das, and A. Bhattacharya, "Push-pull inverter based wireless power transfer system," in *Proceedings of the 7th International Conference on Signal Processing and Integrated Networks (SPIN)*, pp. 489–493, Noida, India, February 2020.

[28] Z. Kaczmarczyk and W. Jurczak, "A push-pull class-E inverter with improved efficiency," *IEEE Transactions on Industrial Electronics*, vol. 55, no. 4, pp. 1871–1874, 2008.

[29] E. Babaei, E. Shokati Asl, and M. Hasan Babayi, "Steady-state and small-signal analysis of high-voltage gain half-bridge switched boost inverter," *IEEE Transactions on Industrial Electronics*, vol. 63, no. 6, pp. 3546–3553, 2016.

[30] S.-H. Ryu, D.-G. Woo, M.-K. Kim, and B.-K. Lee, "Analysis and design of modified half-bridge series-resonant inverter with DC-link neutral-point-clamped cell," *IEEE Transactions on Power Electronics*, vol. 31, no. 3, pp. 2282–2295, 2016.

[31] L. Zhang, K. Sun, Y. Xing, and J. Zhao, "A family of five-level dual-buck full-bridge inverters for grid-tied applications," *IEEE Transactions on Power Electronics*, vol. 31, pp. 7029–7042, 2016.

[32] X. Liu, G. Ma, P. R. Pagilla, and S. S. Ge, "State-estimator-based asynchronous repetitive control of discrete-time markovian switching systems," *Complexity*, vol. 2020, Article ID 6195162, 13 pages, 2020.

[33] R. Yi and C. Boshi, *Electric Drive Automatic Control System-Motion Control System*, pp. 70-71, China Machine Press, Beijing, China, 2009.

[34] J. Na, X. Ren, R. Costa-Castelló, and Y. Guo, "Repetitive control of servo systems with time delays," *Robotics and Autonomous Systems*, vol. 62, no. 3, pp. 319–329, 2014.

[35] R. Griñó and R. Costa-Castelló, "Digital repetitive plug-in controller for odd-harmonic periodic references and disturbances," *Automatica*, vol. 41, no. 1, pp. 153–157, 2005.

[36] R. Costa-Castello, J. Nebot, and R. Grino, "Demonstration of the internal model principle by digital repetitive control of an educational laboratory plant," *IEEE Transactions on Education*, vol. 48, no. 1, pp. 73–80, 2005.

[37] W. S. Chang, I. H. Suh, and T. W. Kim, "Analysis and design of two types of digital repetitive control systems," *Automatica*, vol. 31, no. 5, pp. 741–746, 1995.

[38] M. Steinbuch, "Repetitive control for systems with uncertain period-time," *Automatica*, vol. 38, no. 12, pp. 2103–2109, 2002.

[39] T. Inoue, "Practical repetitive control system design," in *Proceedings of the 29th IEEE Conference on Decision and Control*, pp. 1673–1678, Honolulu, HI, USA, December 1990.

[40] R. Costa-Castello, G. A. Ramos, J. M. Olm, and M. Steinbuch, "Second-order odd-harmonic repetitive control and its

application to active filter control," in *Proceedings of the IEEE Conference on Decision & Control*, Atlanta, GA, USA, December 2011.